https://doi.org/10.1007/s11467-024-1409-4

RESEARCH ARTICLE

Strain-engineered rippling at the bilayer-MoS_2 interface identified by advanced atomic force microscopy

Haoyu Dong[1,2,*], Songyang Li[1,2,*], Shuo Mi[1,2], Jianfeng Guo[1,2], Zhaxi Suonan[1,2], Hanxiang Wu[1,2], Yanyan Geng[1,2], Manyu Wang[1,2], Huiwen Xu[1,2], Li Guan[3], Fei Pang[1,2], Wei Ji[1,2], Rui Xu[1,2,†], Zhihai Cheng[1,2,‡]

[1]Beijing Key Laboratory of Optoelectronic Functional Materials & Micro-nano Devices, Department of Physics, Renmin University of China, Beijing 100872, China

[2]Key Laboratory of Quantum State Construction and Manipulation (Ministry of Education), Renmin University of China, Beijing 100872, China

[3]Key Laboratory of Advanced Light Conversion Materials and Biophotonics, Department of Chemistry, Renmin University of China, Beijing 100872, China

*These authors contributed equally to this work.

Corresponding authors. E-mail: †ruixu@ruc.edu.cn, ‡zhihaicheng@ruc.edu.cn

Supplementary Information

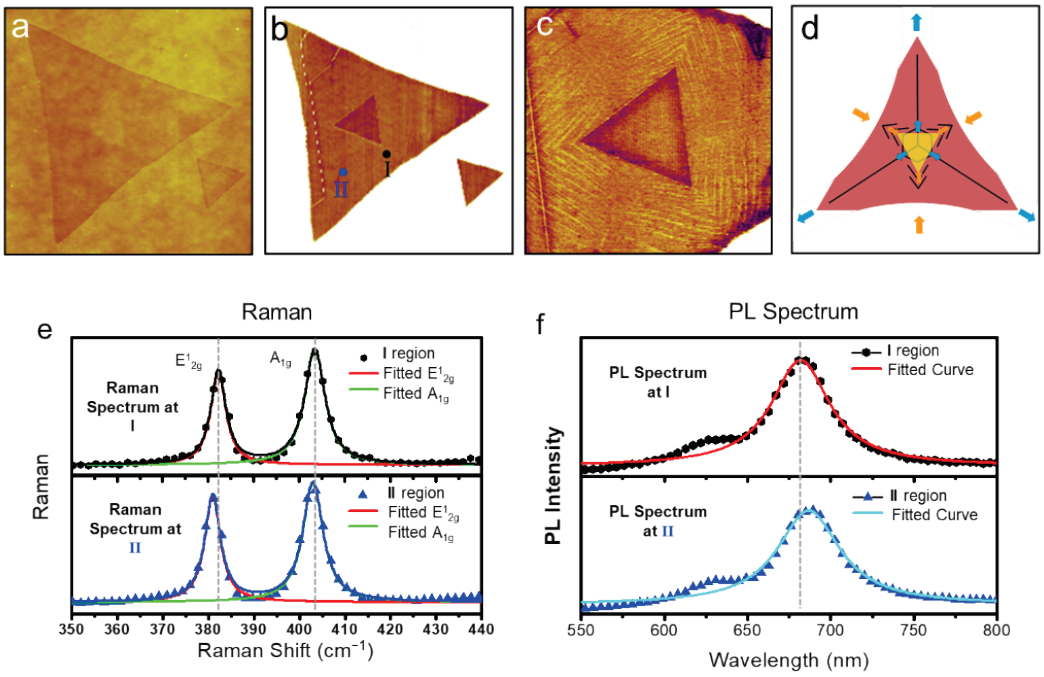

Fig. S1 Raman and PL spectra of MoS_2 in the manuscript. The AFM topography **(a)** and corresponding FFM friction **(b)** images of 2H-MoS_2 bilayer flake on the SiO_2/Si substrates. **(c)** The zoom-in image of (b) at the central region. **(d)** Schematic formation mechanism for the strain-engineered triangular 2H-MoS_2 bilayer flake. It is noted that the central top layer of 2H-MoS_2 is under the interfacial compression via the compressive bottom layer. **(e)** Raman spectra of 1L-MoS_2. **(f)** PL spectra of 1L-MoS_2, I and II are marked in (b).

We preformed Raman and PL measurement of 1L-MoS_2 in the manuscript, as shown in Figs. S1(e) and (f). The A_{1g} mode is less affected in terms of softening and broadening of the peak than the E^1_{2g} mode. In contrast to the unstrained MoS_2 layers, the E^1_{2g} mode of I and II regions is shifted toward lower frequencies. The PL peak exhibits a redshift (i.e., smaller bandgap) with respect to the unstrained MoS_2 monolayer, as shown in Fig. S1(f). As shown in

Fig. S1(b), region I is experiencing compressive stress while region II is undergoing tensile stress. According to Raman and PL results, the variation of region I and II are very small [1], estimated at only about 1%.

We also performed Raman and PL characterization of 2L-MoS_2 rippling, and we found that the characterization results were consistent with the pristine MoS_2 results. This is because the strain of the 2L-MoS_2 is too small, which is less than the limit of Raman resolution and cannot be detected by Raman measurements.

The rippling was observed only in our bimodal AFM images in Fig. S1(c), not in the topography images of Fig. S1(a). This is because the height of rippling structure is very small, which is less than AFM topography limit (20pm), so we can estimate that the height of this rippling structure is smaller than 20pm. Considering the wavelength of rippling structure is about 300 nm, we can determine their strain is very small (less than 1/1000). This ratio is extremely small and necessitates precise detection methods for characterization. In both this manuscript and our previous work [3, 4], we have successfully identified structures in small strain through sophisticated FFM and bimodal AFM techniques, which highlights the advantage of our advanced AFM method.

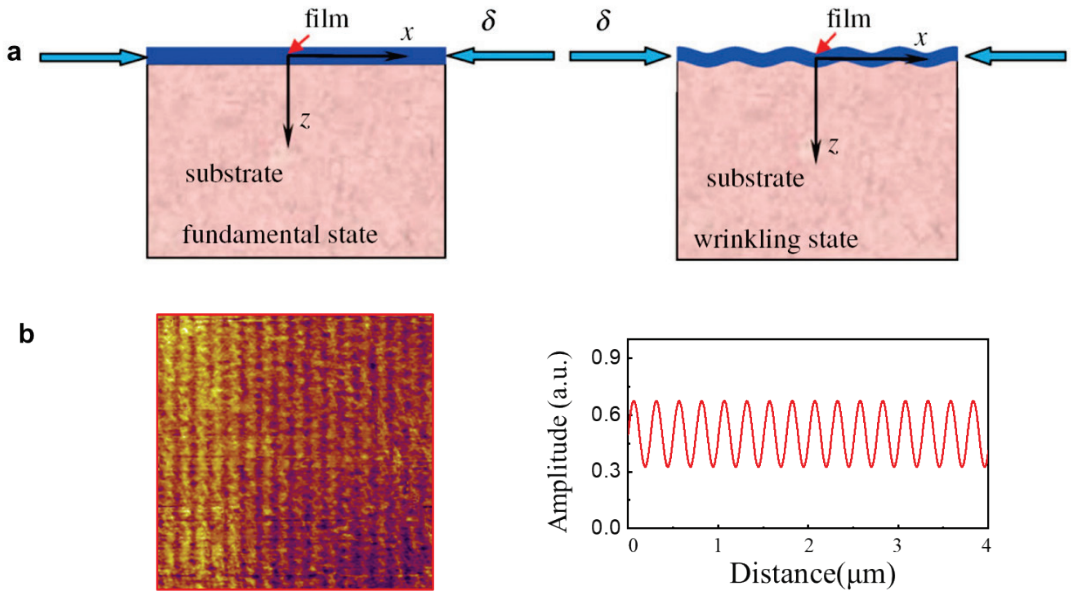

Fig. S2 Surface wrinkling/rippling in the film/substrate bilayer system. **(a)** Schematic of compression induced surface wrinkling/rippling in the film/substrate bilayer system. **(b)** FFM image and corresponding line profile of the rippling structure. Figure (a) was cited from Ref. [5].

In this manuscript, the bilayer MoS_2 on the SiO_2/Si can be simplified to the film/substrate bilayer system. The SiO_2/Si and 1L-MoS_2 was considered as the substrate and the 2L-MoS_2 was considered as the film, as illustrated in Fig. S2(a). The film/substrate bilayer system can be described by the surface wrinkling/rippling model. Consider a flat film under compressive strain, it will become a wrinkling/rippling state. This results in a strain variation in the film as [6]

$$\varepsilon = \frac{2A^2\pi^2}{L^2} \tag{1}$$

and the strain relaxation energy per wave period can be calculated as

$$\Delta U_{strain} = \left(-\frac{\pi^2 A^2 E\varepsilon}{L} + \frac{3\pi^4 A^4 E}{4L^3} \right) Wh \quad , \tag{2}$$

where ε is the compressive strain, A is the amplitude, L is the wavelength, E is the elastic modulus, W is the width of the film, and h is the thickness of the film, respectively.

The observed rippling structure in Fig. S2(b) is similar to the surface wrinkling /rippling model. In the rippling structure of our manuscript, A can be considered as the amplitude of the rippling structure, E is the elastic modulus of MoS_2, h can be considered as the height of single-layer MoS_2. According to the surface wrinkling/rippling model, the ε and ΔU_{strain} in the rippling structure are both very small.

Considering that the surface wrinkling/rippling model is often used to describe systems at mesoscale, the film is much thicker than the rippling structures in this manuscript. As a result, the surface wrinkling/rippling model is not an accurate model to quantitative analysis the rippling structure in this manuscript.

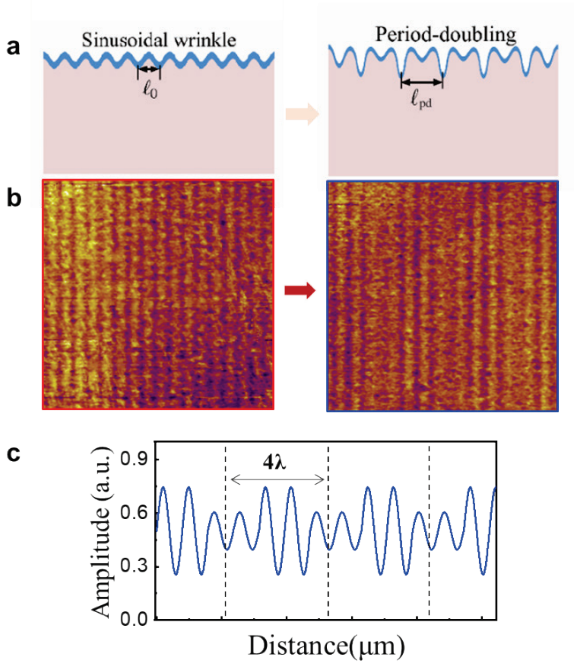

Fig. S3 Period-doubling of surface wrinkling/rippling. **(a)** Schematic of transformation from sinusoidal wrinkle to period-doubling structure. **(b)** FFM images of rippling structures before and during the repeated scanning in the manuscript. **(c)** Line profile of rippling structure (λ_B=4λ) in (b). Figure (a) was cited from reference [7].

The rippling features induced by the repeated contact mode scanning is phenomenally similar to the period-doubling mode in mechanics [7–9]. According to recent research, the experiments show that the sinusoidal wrinkling mode will transform to the period-doubling mode when the overall compressive strain become larger, as shown in Fig. S3(a). This phenomenon was also recently confirmed by nonlinear finite-element simulations [10].

After a careful analysis, we have found that the rippling features induced by the scanning are not exactly the same as the period-doubling mode, as depicted in Fig. S3(c). The rippling structure exhibits two higher peaks and two lower peaks within each period, whereas the period-doubling mode exhibit two equally elevated peaks. Therefore, this period-doubling mode is only phenomenologically similar to the rippling features induced by the repeated scanning and cannot be used to accurately describe it.

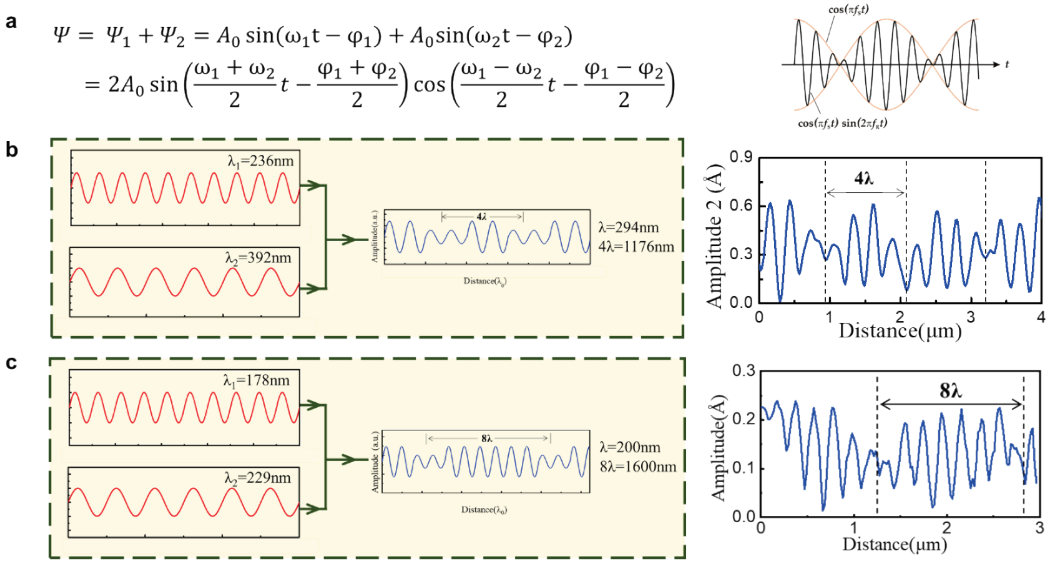

Fig. S4 The beating-like description of the observed rippling structures. **(a)** The formula and schematic of the beating-like rippling structure. **(b)** Formation of the beating-like rippling structure in 2H-MoS_2 (λ_B=4λ). **(c)** Formation of the beating-like rippling structure in 3R-MoS_2 (λ_B=8λ).

These novel rippling structures are discovered for the first time and not been described before. After careful analysis, we find that the rippling structures in the manuscript can be phenomenally described by the beating-like feature.

When two plane waves propagate in the same direction and vibrate in unison, with identical amplitudes but slightly differing frequencies, the phenomenon of the amplitude fluctuating occurs, which is known as the "beat" phenomenon. Their superposition results in waves that exhibit the characteristics of Fig. S3(a), where A_0 is amplitudes of waves, ω_1, φ_1 and ω_2, φ_2 are the circular frequency of waves. Relative to their own frequencies, the difference in frequency between the two waves is minimal.

In this work [Figs. 4(j) and (l)], the “beat”-like rippling structures can be regarded as strain-engineered structure generated by the superposition of stress waves with different wavelengths as shown in Fig. S3(b). Considering the wavelengths of the rippling structure in the initial state [Figs. 4(i) and (k)] λ_1=236 nm, we found that the introduction of a stress wave with a wavelength of λ_2=392 nm can well describe the generation of beat-like structures of 2H-MoS_2 in Fig. S3(b). Similar result of 3R-MoS_2 are shown in Fig. S3(c), the rippling structure can be considered as the result of superposition of two waves with wavelengths λ_1 and λ_2, which exhibits six higher peaks and two lower peaks within each period.

The beating-like phenomenon can only give a phenomenally explanation of the rippling structure. The formation mechanism and accurate description of this rippling structure remains unclear. These questions are interesting and important, but there is currently no theory that can describe them well at the microscale. Considering that our work mainly focuses on the characterization measurement of advanced AFM techniques, it is not discussed in more detail in this manuscript. We will cooperate with mechanics researchers to further investigate the in-depth theory in the following research.

References

1. W. S. Yun, et al., Thickness and strain effects on electronic structures of transition metal dichalcogenides: 2H-MX_2 semiconductors (M = Mo, W; X = S, Se, Te), *Phys. Rev. B* 85, 033305 (2012)
2. C. H. Chang, Orbital analysis of electronic structure and phonon dispersion in MoS_2, $MoSe_2$, WS_2, and WSe_2 monolayers under strain, *Phys. Rev. B* 88, 195420 (2013)
3. S. Hussain, et al., Strain-induced hierarchical ripples in MoS_2 layers investigated by atomic force microscopy, *Appl. Phys. Lett.* 117, 153102 (2020)
4. L. Lei, et al., Size-dependent strain-engineered nanostructures in MoS_2 monolayer investigated by atomic force microscopy, *Nanotechnology* 32, 465703 (2021)
5. Y. Zhao, et al., Towards a quantitative understanding of period-doubling wrinkling patterns occurring in film/substrate bilayer systems, *Proc. R. Soc. A* 471, 20140695 (2014)
6. Y. Zhang, et al., Effect of surface bonding on semiconductor nanoribbon wiggling structure, *Appl. Phys. Lett.* 96, 111904 (2010)
7. Z. Cheng, et al., Intricate evolutions of multiple-period post-buckling patterns in bilayers, *Sci. China-Phys. Mech. Astron.* 64, 214611 (2021)
8. Y. Zhao, et al., Towards a quantitative understanding of period-doubling wrinkling patterns occurring in film/substrate bilayer systems, *Proc. R. Soc. A* 471, 20140695 (2014)
9. F. Brau, et al., Multiple-length-scale elastic instability mimics parametric resonance of nonlinear oscillators, *Nat. Phys.* 7, 56 (2011)
10. Y. P. Cao, et al., Wrinkling phenomena in neo-Hookean film/substrate systems, *J. App. Mech.* 79, 031019 (2012)